Quantitative trait loci mapping and candidate gene analysis of stoma-related traits in wheat (*Triticum aestivum* L.) glumes

Ning Li[1], Fanfan Dong[1], Tongtong Liu[2], Jinwen Yang[1], Yugang Shi[1], Shuguang Wang[1], Daizhen Sun[1] and Ruilian Jing[3]

[1] College of Agronomy, Shanxi Agricultural University, Taigu, China
[2] College of Food Science and Engineering, Shanxi Agricultural University, Taigu, China
[3] National Key Facility for Crop Gene Resources and Genetic Improvement/Institute of Crop Sciences, Chinese Academy of Agricultural Sciences, Beijing, China

ABSTRACT

The photosynthesis of wheat glumes makes important contributions to the yield. Stomata play a crucial role in regulating photosynthesis and transpiration in plants. However, the genetic base of wheat glume stomata is not fully understood. In this study, stomatal length (SL), stomatal width (SW), stomatal density (SD), potential conductance index (PCI) of stomata, stomatal area (SA), and stomatal relative area (SRA) were measured in different parts of wheat glumes from a doubled haploid (DH) population and their parents. Quantitative trait loci (QTLs) of these traits were anchored on a high-density genetic linkage map of the DH population. A total of 61 QTLs for stoma-related traits were mapped onto 16 chromosomes, and each one accounted for 3.63 to 19.02% of the phenotypic variations. Two QTL hotspots were detected in two marker intervals, AX-109400932∼AX-110985652 and AX-108972184∼AX-108752564, on chromosome 6A. Five possibly candidate genes (*TraesCS6A02G105400*, *TraesCS6A02G106400*, *TraesCS6A02G115100*, *TraesCS6A02G115400*, and *TraesCS6A02G116200*) for stoma-related traits of wheat glumes were screened out , according to their predicted expression levels in wheat glumes or spikes. The expression of these genes may be induced by a variety of abiotic stresses. These findings provide insights for cloning and functional characterization of stoma-related candidate genes in wheat glumes.

Subjects Agricultural Science, Genetics, Molecular Biology, Plant Science
Keywords Wheat (*Triticum aestivum L.*), Glume, Stomata, QTL, Candidate gene

Submitted 13 January 2022
Accepted 22 March 2022
Published 8 April 2022

Corresponding author
Daizhen Sun, sdz64@126.com

Academic editor
Robert Winkler

Additional Information and Declarations can be found on page 16

DOI **10.7717/peerj.13262**

INTRODUCTION

Stomata are the main portals for the exchange of gas and water between plants and the external environment (*Li et al., 2017*), and they play an extremely important role in the life activities of plants. Plants optimise their photosynthesis and transpiration rates through regulating the aperture, density, and distribution of stomata when they are stressed by biotic or abiotic factors (*Doheny-Adams et al., 2012*; *Franks et al., 2015*). In addition to spreading a large number on the leaves, stomata also exist on the epidermis of certain

non-foliar organs, such as pods of soybean and oilseed rape, corn bracts, and ears of wheat. (*Wang, Wei & Zheng, 2001*; *Kong et al., 2010*).

Previous studies have reported that leaves are the main organs for plant photosynthesis to generate energy, and the photosynthesis of wheat flag leaves has always been regarded as the main source of assimilation during the filling process (*Maydup et al., 2010*). However, as scientists continue to deepen the research on plant photosynthesis, more and more results showed that the photosynthesis of plant non-foliar organs also plays an important role in the accumulation of carbon assimilates (*Sánchez-Díaz et al., 2002*; *Zhu et al., 2009*; *Sánchez-Bragado et al., 2014*). Compared with leaves, ear organs have unique advantages: for example, the photosynthetic products of wheat ears can be directly transported to the grain, thus avoiding unnecessary energy waste. Wheat ears carry out the C_4 metabolic pathway, which can re-fix the CO_2 produced by photorespiration (*Knoppik, Selinger & Ziegler-Jöns, 1986*; *Araus et al., 1993*). Wheat spikes have stronger drought tolerance, higher osmotic adjustment ability, and water use efficiency (WUE) (*Tambussi & Nogues, 2005*). Compared with lower organs such as flag leaves, wheat spikes age more slowly (*Tambussi et al., 2007*). Thus, wheat ear photosynthesis also makes an important contribution to the yield (*Araus et al., 1993*; *Abbad et al., 2004*; *Zhou et al., 2014*).

Glumes are the main photosynthetic organs of the ear and are believed to be an important source of assimilates for kernel filling in wheat (*Araus et al., 1993*). Glumes can recycle the CO_2 respired by developing grains during photosynthesis and have higher ribulose-1,5-bisphosphate carboxylase (RuBPC, EC 4.1.1.39) activity compared with other ear elements (*Gebbing & Schnyder, 2001*; *Aliyev, 2012*; *Sánchez-Bragado et al., 2014*). It has been reported that glumes actively participate in the process of CO_2 assimilation during kernel filling (*Lopes et al., 2006*). In addition, glumes maintain a higher relative water content and WUE under progressive waterlogging and drought stress than flag leaves, contributing significantly to grain filling (*Rubén et al., 2018*; *Wardlaw, 2002*). Therefore, compared with other organs, glumes may have a higher ability to resist abiotic stress.

So far, many reports on genetic analysis of stoma-related traits have focused on plant leaves, especially in rice. *Teng et al. (2004)* detected one QTL that controls the stomatal conductance of rice leaves at the peak tillering stage on chromosome 4. *Ishimaru et al. (2001)* used a population of crosses between japonica and indica to detect a QTL that controls the stomatal density on the leaf surface and a QTL that is related to the stomatal density on the back of the leaf. Ten QTLs for stomatal density and four QTLs for stomatal size were detected across growth stages and leaf surfaces (adaxial and abaxial) (*Laza et al., 2010*). In wheat, twenty QTLs for stomatal density and size of leaves were identified under drought stress (*Wang et al., 2016*). However, genetic analysis of stoma-related traits in wheat glumes is rarely reported.

In this study, stomatal density, length, and width on the top, middle, and base of wheat glumes were measured and the potential conductance index of stomata, stomatal area, and stomatal relative area in different parts of glumes were calculated. A high-density linkage genetic map was used for QTL mapping of stoma-related traits and the candidate genes related were screened. These QTLs and candidate genes will provide insights for studying the molecular mechanism of stomatal development of the wheat ear.

MATERIALS & METHODS

Test material

A wheat double haploid (DH) population (*Liu et al., 2013*), including 150 lines that derived from a cross between Hanxuan 10 and Lumai 14 was used in this study. All the 150 lines and parents were grown at the experimental farm (37°25′N, 112°35′E) of Shanxi Agricultural University in 2018 and 2019. The field experiments were conducted by randomized complete block design (RCBD) with three replicates. Each plot consisted of two rows of 2 m in length, with 0.25 m between rows. Water and fertilizer management during the growth period was complied with the local production practice.

Measurement and calculation of stomata-related traits in glumes

For each DH line and parents, three flowering plants with consistent growth were tagged. The middle spikes of the three plants were quickly placed into a 2-mL centrifuge tube with FAA solution (formalin: acetic acid: 70% alcohol = 1:1:18) three days after anthesis, respectively. The sampling was started at 10 am on the third day after anthesis. The average temperature at the time of sampling was 13 and 17 °C, and the moisture content of topsoil (0∼30 cm) was approximately 15% and 13% (v/v) in 2018 and 2019, respectively. Stomatal density (SD), stomatal length (SL), and stomatal width (SW) on the top, middle, and base of wheat glumes were measured as previously described in *Wang et al. (2018)*.

Calculations of other stoma-related traits were as follows:

Potential conductance index (PCI) = $SL^2 \times SD \times 10^{-4}$ (*Nicholas & Richardson, 2009*)

Stomatal area (SA) = $\pi \times 1/2$ SL $\times$ 1/2 SW (*Robert, Gretchen & Richard, 2000*)

Stomatal relative area (SRA) = SD $\times$ SA $\times 10^{-4}$ (*Sun et al., 2021*)

Data analysis

The relevant *t*-test and analysis of variance (ANOVA) were carried out by the statistical software package SPSS v.17.0; the frequency distribution map was generated by Excel 2007; and the phenotypic correlation analysis map was created in the R-package corrplot (*Wei & Simko, 2013*).

QTL mapping

The genetic map of the DH population was constructed by Jing Ruilian's team at the Institute of Crop Science, Chinese Academy of Agricultural Sciences (*Li et al., 2019*). The linkage map is 4,082.4 cM in length and contains 1630 SNP and 224 SSR markers, with 2.2 cM per bin on average (*Shi et al., 2020*). QTL mapping was performed as previously described in *Li et al. (2021)* using the IciMapping 4.1 software. The LOD score for declaring a QTL was 2.5 for each trait.

Prediction of candidate genes

Candidate genes in associated loci were predicted according to the reference genome sequence of 'Chinese Spring' wheat (*IWGSC RefSeqv1.1*) published by the International Wheat Genome Sequencing Consortium. Gene annotation was carried out by referring to the Ensembl Plants database (https://plants.ensembl.org/index.html). We used a publicly

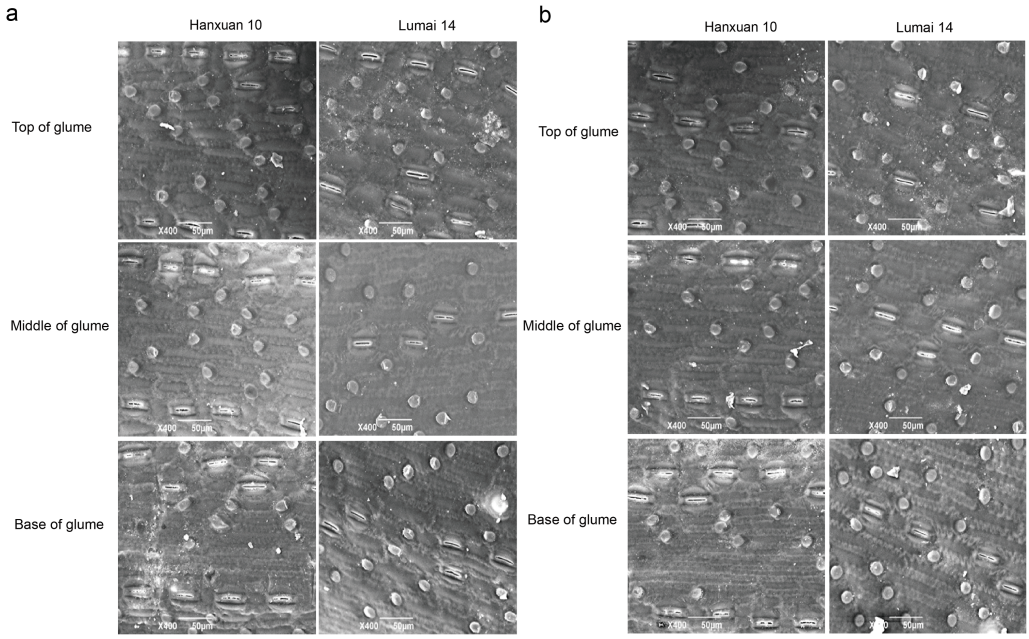

Figure 1 **Distribution of stomata in different parts of wheat glumes observed in 2018 (A) and 2019 (B).**
Full-size DOI: 10.7717/peerj.13262/fig-1

available database, WheatOmics (http://wheatomics.sdau.edu.cn/) (*Ma et al., 2021*), to obtain the expression profiles of all candidate genes.

RESULTS

Phenotypic variation of glume stoma-related traits in the DH population and parents

We observed regular rows of stomata on the top, middle, and base of glumes in parents (Fig. 1). SD of different parts of glumes in Lumai 14 showed significant or highly significant differences between the two years, while Hanxuan 10 had a significant difference in SD only at the base of glumes (Table 1). For DH lines, except for SD at the base of glumes, the phenotypic values of SD of other parts of glumes in 2019 were significantly lower than those in 2018 (Table 1). These results indicated that SD of glumes is greatly affected by the environment, and this phenomenon is more obvious in Lumai 14 than Hanxuan 10. In general, from the top to the base, SD of glumes gradually became less (Table 1).

Except for the middle of glumes in Hanxuan10, differences in SL of the rest parts of glumes between the two years were not significant in the two parents. Except for the top of glumes of Lumai 14, differences in SW of the rest parts of glumes between the two years were not significant in the two parents. For the DH lines, the difference in SL of glumes was not significant between the two years, but SW in 2019 was highly significantly smaller than that in 2018 (Table 1). These results indicated that SW of glumes is more affected by the environment than SL. For the 150 DH lines, there were genetic differences in the same stoma-related traits among different lines, and this difference varied among different traits. The coefficient of variation of SD in the DH population was greater than 10 in both 2018

Table 1 Phenotypic variation of stoma-related traits of wheat glumes in the DH population and parents.

Traits[a]	Environments	Parents		Difference[c]	DH lines						
		Hanxuan10[b]	Lumai14[b]		Min	Max	Mean[b]	SD	Skewness	Kurtosis	CV
SDt (No./mm^2)	2018	89.79a/A	81.63a/A	8.16*	60.21	111.44	85.43a/A	10.50	−0.37	0.81	12.29%
	2019	88.15a/A	74.12b/B	14.03**	59.41	106.87	78.99b/B	8.95	−0.91	3.67	11.33%
SDm (No./mm^2)	2018	80.27a/A	77.16a/A	3.15	52.03	112.20	78.33a/A	10.42	0.28	0.26	13.30%
	2019	82.17a/A	61.49b/B	20.68**	50.24	94.47	73.56b/B	9.14	−0.85	2.11	12.42%
SDb (No./mm^2)	2018	75.35b/A	74.01a/A	1.34	43.54	105.46	72.38a/A	10.92	0.16	0.34	15.08%
	2019	82.05a/A	63.13b/A	18.92**	40.01	103.90	69.17a/A	11.08	−0.31	1.98	16.02%
SLt (μm)	2018	45.60a/A	47.58a/A	−1.98	39.76	50.83	45.71a/A	2.42	−0.17	−0.61	5.29%
	2019	45.08a/A	45.19a/A	−0.11	40.03	50.25	45.67a/A	2.07	−0.16	−0.51	4.53%
SLm (μm)	2018	48.42a/A	46.85a/A	1.57	39.19	51.76	45.99a/A	2.32	−0.09	−0.23	5.04%
	2019	44.50b/A	46.75a/A	−2.25*	40.11	50.97	46.11a/A	2.24	−0.35	−0.13	4.86%
SLb (μm)	2018	48.73a/A	46.96a/A	1.77	38.33	51.25	45.22a/A	2.59	−0.11	−0.19	5.73%
	2019	45.15a/A	47.06a/A	−1.91*	38.63	50.50	44.70a/A	2.40	−0.03	−0.50	5.37%
SWt (μm)	2018	27.47a/A	34.55a/A	−7.08**	24.65	36.50	29.21a/A	2.42	1.06	2.23	8.28%
	2019	30.18a/A	28.93b/A	1.25	25.10	33.54	27.65b/B	1.29	1.28	3.08	4.67%
SWm (μm)	2018	30.45a/A	30.80a/A	−0.35	25.53	35.54	29.57a/A	2.22	0.86	1.02	7.51%
	2019	29.03a/A	29.55a/A	0.52	24.72	33.00	27.86b/B	1.58	0.53	0.64	5.67%
SWb (μm)	2018	30.80a/A	31.53a/A	−0.73	24.83	35.91	29.34a/A	2.48	0.79	1.08	8.45%
	2019	29.45a/A	32.36a/A	−2.91*	23.82	34.38	27.59b/B	1.88	0.95	1.40	6.81%
PCIt	2018	19.67a/A	17.91a/A	1.76	9.95	23.49	17.79 a/A	2.20	−0.04	1..01	12.37%
	2019	17.74a/A	14.88a/A	2.86	5.78	22.31	16.45 a/A	1.89	−0.77	2.78	11.49%
PCIm	2018	17.82a/A	16.77a/A	1.05	9.55	22.93	16.51 a/A	2.01	0.18	1.20	12.17%
	2019	16.31a/A	13.22b/B	3.09*	5.51	19.93	15.60 a/A	1.96	−0.76	1.97	12.56%
PCIb	2018	17.79a/A	16.40a/A	1.39	7.63	21.51	14.75 a/A	2.24	0.09	0.62	15.18%
	2019	16.53a/A	13.75a/A	2.78**	4.86	23.28	13.79 a/A	2.30	−0.04	1.58	16.68%
SAt (μm^2)	2018	1123.29a/A	1032.60a/A	90.69*	849.26	1397.99	1050.23 a/A	109.82	0.65	0.65	10.46%
	2019	1021.78a/A	986.60a/A	35.18	830.49	1258.00	991.41 a/A	65.37	0.48	1.21	6.59%
SAm (μm^2)	2018	944.15a/A	979.19a/A	−35.04	861.54	1460.76	1069.71 a/A	102.88	0.50	0.85	9.62%
	2019	996.95a/A	1043.27a/A	−46.32**	818.67	1306.33	1009.14 a/A	83.93	0.44	0.84	9.47%
SAb (μm^2)	2018	1135.79a/A	1120.20a/A	15.59	799.39	1412.54	1044.39 a/A	119.29	0.61	0.36	8.32%
	2019	975.76a/A	1153.63a/A	−177.87**	784.21	1203.87	968.12 b/B	85.79	0.31	−0.40	8.86%

(*continued on next page*)

Table 1 (*continued*)

Traits[a]	Environments	Parents		Difference[c]	DH lines						
		Hanxuan10[b]	Lumai14[b]		Min	Max	Mean[b]	SD	Skewness	Kurtosis	CV
SRAt (%)	2018	9.96a/A	8.31a/A	1.65	4.56	12.16	8.94 a/A	1.20	0.01	0.74	13.42%
	2019	8.89a/A	7.23b/B	1.66	2.77	9.72	7.81 b/B	0.86	−0.96	2.74	11.01%
SRAm (%)	2018	9.09a/A	6.82a/A	2.27*	4.59	12.16	8.36 a/A	1.25	0.44	0.85	14.95%
	2019	8.08a/A	6.30b/A	1.78	2.62	10.24	7.40 a/A	0.97	−0.58	1.75	13.11%
SRAb (%)	2018	8.65a/A	8.52a/A	0.13	4.35	12.16	7.54 a/A	1.31	0.48	0.85	17.37%
	2019	7.96a/A	7.17a/A	0.79	2.34	11.79	6.68 b/A	1.17	0.25	1.91	17.51%

Notes.

[a]SD, stomatal density; SL, stomatal length; SW, stomatal width; PCI, potential conductance index; SA, stomatal area; SRA, stomatal relative area; t, top of glumes; m, middle of glumes; b, base of glumes.

[b]Different letters after the values in a column indicate significant differences between two years.

[c]Asterisks (* and **) indicate significance at p-value < 0.05 and p-value < 0.01, respectively.

and 2019, while the coefficient of variation of both SL and SW was less than 10. This also showed that different stomatal-related traits are affected differently by the environment. In addition, SL and SW did not change significantly from the top to the base of wheat glumes.

Except for the middle of glumes of Lumai 14, differences in stomatal PCI of the rest parts of glumes between the two years were not significant in the two parents. Differences in stomatal PCI of all parts between the two years were not significant for the DH lines neither. Differences in SA of all parts between the two years were not significant in the two parents. Except for the top and middle of glumes of Lumai 14, differences in SRA of the rest parts of glumes between the two years were not significant in the two parents (Table 1).

Stoma-related traits of the DH lines showed continuous transgressive segregation with skewness and kurtosis values close to zero, suggesting normal distribution. All target traits were thus quantitatively controlled by multiple genes and were suitable for QTL mapping (Table 1) (Fig. S1).

Correlation between glume stoma-related traits

For all parts of glumes, SD showed a highly significantly negative correlation with SL in 2018 and 2019; however, the correlation between SD and SW was not significant. There was a significantly positive correlation between SL and SW in 2018, but such correlation was not significant in 2019. In addition, SD showed a highly significant and positive correlation with PCI and SRA in 2018 and 2019. SL showed a significantly positive correlation with SA in both years. SW showed a significantly positive correlation with SA and SRA in both years. In 2018, any two of PCI, SA, and SRA were significantly positively correlated, while the degree of correlation was weakened in 2019 (Fig. 2 Table S1).

QTL mapping for traits related to stomata in wheat glumes

A total of 61 QTLs for traits related to stomata of wheat glumes were detected in the two years. The phenotypic variation of these QTLs ranged from 3.63 to 19.02%. The LOD score ranged from 2.51 to 22.12, and the QTLs were distributed on 16 chromosomes including 1A, 1D, 2A, 2B 2D, 3A, 3D, 4B, 5A, 5B, 5D, 6A, 6B, 7A, 7B, and 7D, respectively (Fig. 3 Table 2). A total of nine QTLs were detected in both years.

A total of 10 QTLs corresponding to SD of glumes were detected in the two years. The phenotypic variation of these QTLs ranged from 6.78 to 11.41%. Among these QTLs, *QSDt-2A* was detected in both years; *QSDt-5A* and *QSDm-5A* were detected in the same interval in 2018. Twenty-one QTLs were associated with stomatal size and detected in both years. Among these QTLs, *QSLt-2D*, *QSLm-7A*, and *QSLb-6A-1* were detected in both years. *QSLb-6A-2* and *QSWb-6A* were detected in the same interval in 2019. A total of 30 QTLs associated with PCI, SA, and SRA were detected in the two years. Among these QTLs, *QPCIb-6A-1*, *QSAt-2D*, *QSAm-3A*, and *QSRAb-6A-2* were detected in the two years. Among all QTLs, *QSRAb-6A-1* had the largest LOD value (22.12) (Fig. 3 Table 2).

Among all QTLs, two QTL hotspots were found on chromosome 6A. One was in the interval AX-109400932∼AX-110985652, which contained four QTLs related to SL, SD, PCI, and SRA in the two years. The other was in the interval AX-108972184∼AX-108752564, which contained four QTLs related to SW, SD, PCI, and SRA in the two years (Fig. 3 Table 2).

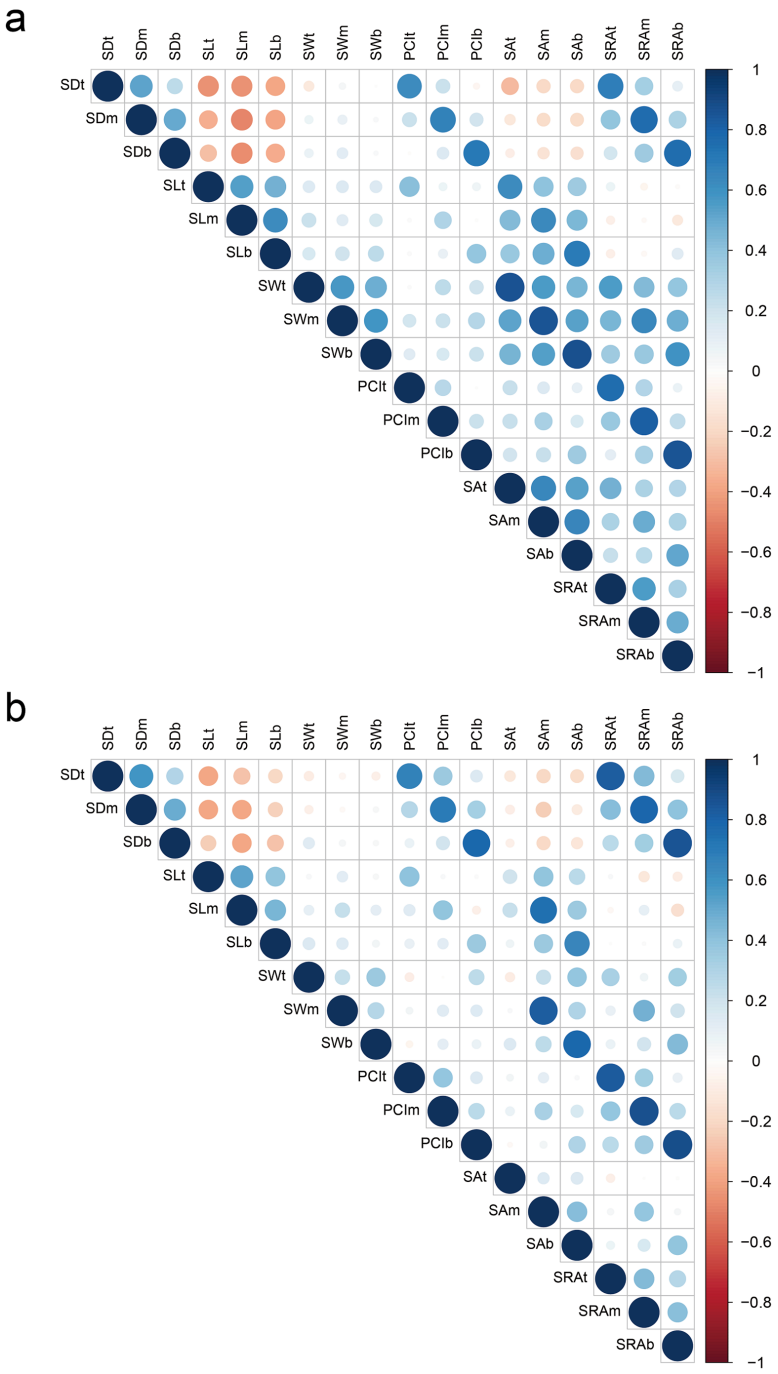

Figure 2 Correlation of stoma-related traits in 2018 (A) and 2019 (B). Red and blue colors indicate significantly positive and negative correlations, respectively, whereas white color indicates no significant correlation. SD, stomatal density; SL, stomatal length; SW, stomatal width; PCI, potential conductance index; SA, stomatal area; SRA, stomatal relative area; t, top of glumes; m, middle of glumes; b, base of glumes.
Full-size DOI: 10.7717/peerj.13262/fig-2

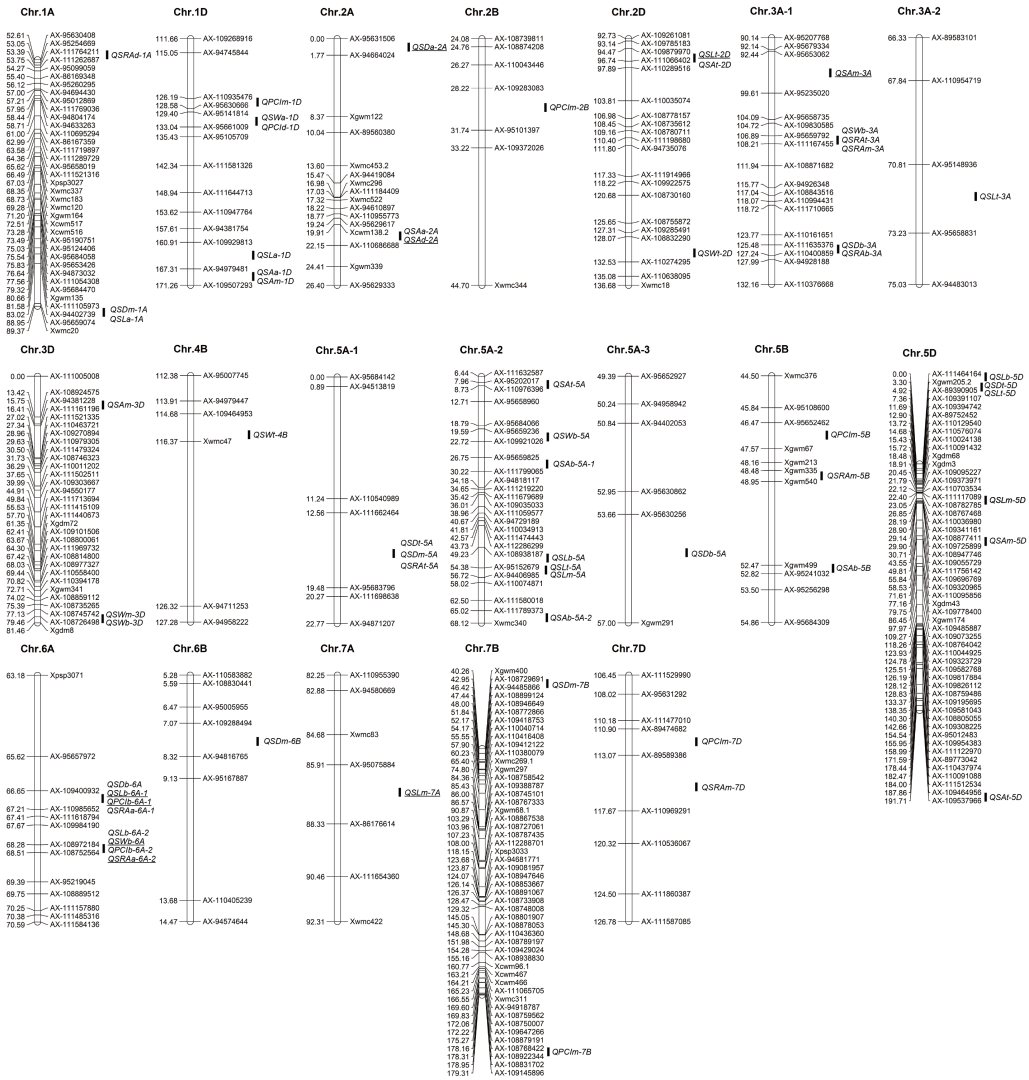

Figure 3 **Distribution of QTLs for stoma-related traits on a high-density linkage map.** To better display the QTLs, the high-density linkage maps show only markers near the QTL intervals. The QTLs with underscore indicate that they were detected in both years.

Full-size DOI: 10.7717/peerj.13262/fig-3

The prediction of candidate genes

For the first QTL hotspot, the physical positions of the two markers AX-109400932 and AX-110985652 were 73571398 and 76990896 bp, respectively. According to the reference genome sequence of 'Chinese Spring' wheat (*IWGSC RefSeqv1.1*), a total of 33 genes were found between the two markers, and gene annotation was carried out by referring to the Ensembl Plants database (Table S2). For the other QTL hotspot, the physical positions of the two markers AX-108972184 and AX-108752564 were 83931623 and 86272494 bp, respectively, covering a total of 24 genes (Table S2). Using WheatOmics, the expression levels of these 57 genes in wheat glumes and spikes were predicted (*The International Wheat Genome Sequencing Consortium IWGSC, 2018*). The results showed that there

were five genes (*TraesCS6A01G105400*, *TraesCS6A01G106400*, *TraesCS6A01G115100*, *TraesCS6A01G115400*, and *TraesCS6A01G116200*) with higher expression levels in wheat glumes or spikes (Fig. 4 Table 3).

Then, the expression levels of these five genes under different abiotic stresses were predicted (*Oono et al., 2013*; *Liu et al., 2015*; *Nazanin et al., 2019*). The results showed that the expression of these genes was induced by different abiotic stresses, and the expression patterns of different genes under the same abiotic stress were also different (Fig. 5). For example, the expression of *TraesCS6A01G105400* was significantly reduced after being subjected to low phosphorus stress in wheat shoots and roots. The expression levels of *TraesCS6A01G115100* and *TraesCS6A01G116200* both increased after being subjected to low phosphorus stress in shoots and roots. The expression of *TraesCS6A01G106400* was only significantly increased in the root after being subjected to low phosphorus stress. The expression level of *TraesCS6A01G105400* was significantly reduced in wheat seedling leaves subjected to drought stress, heat stress, and their combination. The expression levels of *TraesCS6A01G106400* and *TraesCS6A01G116200* were significantly increased after six hours of drought stress, heat stress, and their combination. Among these five genes, only the expression level of *TraesCS6A01G115400* was significantly decreased after being exposed to salt stress (Fig. 5).

DISCUSSION

Phenotypic correlation of stoma-related traits in wheat glumes

Stomata are the channel for water and gas exchange in the process of wheat photosynthesis and respiration, which indirectly affect the yield of wheat (*Berger & Altmann, 2000*). Studies have shown that a variety of environmental factors at different growth and developmental stages of plants can affect the formation of stomata, such as water (*Stephens & Waugh, 2017*), temperature (*Qi & Torii, 2018*), light (*Boccalandro et al., 2009*), and CO_2 concentration (*Hu et al., 2010*). *Aasamaa, Sober & Rahi (2001)* reported that the stomatal length of forest tree species decreased with increasing drought. For some light-loving crops, the formation of stomata can be promoted by increasing the light intensity. In the present study, stomatal density and stomatal width of wheat glumes showed significant differences between the two years, but stomatal length showed no significant differences (Table 1). These results suggest that stomatal length may have higher stability in response to different environmental conditions than stomatal density and width. In addition, we also compared the differences of the same traits in different parts of wheat glumes, and the results showed that from the top to the base of glumes, the stomatal density gradually decreased, but the stomatal length and width did not change significantly. Moreover, four of the nine stable QTLs mapped were associated with stoma-related traits at the base of wheat glumes. It is speculated that this may be because the stomatal properties at the base of the glume are the most stable compared with other parts.

Franks & Beerling (2009) have reported that the negative correlation between stomatal size and stomatal density helps to adjust the plasticity of stomata, thereby regulating the maximal stomatal conductance of wheat. There was a significantly negative correlation

Table 2 Quantitative trait loci (QTLs) for stoma-related traits of wheat glumes in DH population[a].

Trait[b]	Location[c]	QTL[d]	Chr	Left marker	Right marker	2018			2019		
						LOD	PVE (%)	Add	LOD	PVE (%)	Add
SD	Top	*QSDt-2A*	2A	AX-95631506	AX-94664024	3.57	9.60	2.73	2.63	6.92	2.28
		QSDt-5A	5A	AX-111662464	AX-95683796	2.66	8.10	−2.94			
		QSDt-5D	5D	Xgwm205.2	AX-89390905				2.57	6.78	−2.25
	Middle	*QSDm-1A*	1A	AX-111105973	AX-94402739				2.82	8.89	2.66
		QSDm-5A	5A	AX-111662464	AX-95683796	3.77	8.74	3.37			
		QSDm-6B	6B	AX-109288494	AX-94816765				2.56	7.87	−2.47
		QSDm-7B	7B	AX-108729691	AX-94485866	3.02	6.92	−2.97			
	Base	*QSDb-3A*	3A	AX-111635376	AX-110400859	3.44	8.66	−3.37			
		QSDb-5A	5A	AX-95630256	Xgwm291				3.84	11.41	3.76
		QSDb-6A	6A	AX-109400932	AX-110985652				7.27	8.98	3.22
SL	Top	*QSLt-1A*	1A	AX-111105973	AX-94402739	5.60	11.33	−0.90			
		QSLt-1D	1D	AX-109929813	AX-94979481	3.70	7.31	−0.70			
		QSLt-2D	2D	AX-109879970	AX-111066402	5.22	11.06	0.76	4.49	9.26	−0.69
		QSLt-3A	3A	AX-95148936	AX-95658831	4.50	8.93	0.79			
		QSLt-5A	5A	AX-95152679	AX-94406985	3.36	6.55	−0.66			
		QSLt-5D	5D	Xgwm205.2	AX-89390905				2.54	5.45	0.53
	Middle	*QSLm-5A*	5A	AX-95152679	AX-94406985	2.79	5.07	−0.62			
		QSLm-5D	5D	AX-111117089	AX-108782785				2.88	8.68	0.65
		QSLm-7A	7A	AX-95075884	AX-86176614	5.61	10.57	0.96	3.31	6.05	−0.70
	Base	*QSLb-5A*	5A	AX-108938187	AX-95152679	3.26	9.53	−0.81			
		QSLb-5D	5D	AX-111464164	Xgwm205.2				2.94	9.18	0.70
		QSLb-6A-1	6A	AX-109400932	AX-110985652	6.42	9.64	1.17	5.31	8.97	1.01
		QSLb-6A-2	6A	AX-108972184	AX-108752564				6.97	9.59	−1.19
SW	Top	*QSWt-1D*	1D	AX-95141814	AX-95661009	2.83	7.89	−0.69			
		QSWt-2D	2D	AX-108832290	AX-110274295				3.86	11.31	−0.43
		QSWt-4B	4B	AX-109464953	Xwmc47	2.58	7.40	−0.67			
	Middle	*QSWm-3D*	3D	AX-108735265	AX-108745742				2.99	8.91	−0.47
		QSWb-3A	3A	AX-95659792	AX-111167455				2.84	6.94	−0.52
	Base	*QSWb-3D*	3D	AX-108735265	AX-108745742	2.63	10.59	−0.69			
		QSWb-5A	5A	AX-95659236	AX-109921026				3.32	8.19	−0.57
		QSWb-6A	6A	AX-108972184	AX-108752564	3.47	8.74	−0.77	4.29	9.75	−0.77

(*continued on next page*)

Table 2 (*continued*)

Trait[b]	Location[c]	QTL[d]	Chr	Left marker	Right marker	2018			2019		
						LOD	PVE (%)	Add	LOD	PVE (%)	Add
PCI	Middle	*QPCIm-1D*	1D	AX-110935476	AX-95630666				2.65	3.63	−0.44
		QPCIm-2B	2B	AX-109283083	AX-95101397				4.15	5.82	0.57
		QPCIm-5B	5B	AX-95652462	Xgwm67				11.52	19.02	−1.03
		QPCIm-7B	7B	AX-108768422	AX-108922344				3.72	5.19	−0.53
		QPCIm-7D	7D	AX-89474682	AX-89589386				5.26	7.52	−0.64
	Base	*QPCIb-1D*	1D	AX-95141814	AX-95661009				2.71	4.56	−0.59
		QPCIb-6A-1	6A	AX-109400932	AX-110985652	18.42	13.64	3.55	21.79	14.06	3.15
		QPCIb-6A-2	6A	AX-108972184	AX-108752564				17.81	8.65	−2.47
SA	Top	*QSAt-1D*	1D	AX-94979481	AX-109507293	3.86	6.87	−42.97			
		QSAt-2A	2A	Xcwm138.2	AX-110686688	4.12	9.25	−50.09			
		QSAt-5A	5A	AX-95202017	AX-110976396	5.14	9.28	−50.40			
		QSAt-2D	2D	AX-109879970	AX-111066402	5.24	8.73	31.24	8.40	13.96	−38.91
		QSAt-5D	5D	AX-109464956	AX-109537966				2.92	4.45	−22.28
	Middle	*QSAm-1D*	1D	AX-94979481	AX-109507293	4.36	10.99	−43.05			
		QSAm-3A	3A	AX-95653062	AX-95235020	3.68	9.18	−39.55	3.01	7.42	−35.62
		QSAm-3D	3D	AX-94381228	AX-111161196				3.16	9.18	−31.81
		QSAm-5D	5D	AX-108877411	AX-109725899				2.71	7.88	28.75
	Base	*QSAb-5A-1*	5A	AX-95659825	AX-111799065				7.45	13.27	−46.15
		QSAb-2A	2A	Xcwm138.2	AX-110686688				6.14	12.89	−44.81
		QSAb-5A-2	5A	AX-111789373	Xwmc340	2.61	7.88	−42.04			
		QSAb-5B	5B	Xgwm499	AX-95241032				3.81	6.65	−32.36
SRA	Top	*QSRAt-3A*	3A	AX-95659792	AX-111167455	3.20	8.56	−0.35			
		QSRAt-5A	5A	AX-111662464	AX-95683796	3.94	11.30	−0.40			
	Middle	*QSRAm-3A*	3A	AX-95659792	AX-111167455	2.66	10.30	−0.35			
		QSRAm-5B	5B	Xgwm335	Xgwm540				5.15	12.63	−0.36
		QSRAm-7D	7D	AX-89589386	AX-110969291				3.97	9.51	−0.31
	Base	*QSRAb-1A*	1A	AX-111764211	AX-111262687	2.51	7.15	−0.35			
		QSRAb-3A	3A	AX-111635376	AX-110400859	4.58	13.48	−0.46			
		QSRAb-6A-1	6A	AX-109400932	AX-110985652				22.12	10.74	1.68
		QSRAb-6A-2	6A	AX-108972184	AX-108752564	15.31	8.89	−1.39	18.38	6.82	−1.34

Notes.

[a]LOD, LOD value of each QTL; PVE, phenotypic variance explained by QTL; Add, a positive sign means increased effect contributed by Hanxuan 10; a negative sign indicates increased effect contributed by Lumai 14.

[b]SD, stomatal density; SL, stomatal length; SW, stomatal width; PCI, potential conductance index; SA, stomatal area; SRA, stomatal relative area.

[c]Top, top of glumes; Middle, middle of glumes; Base, base of glumes.

[d]Underlined QTLs indicate that they were detected in two years.

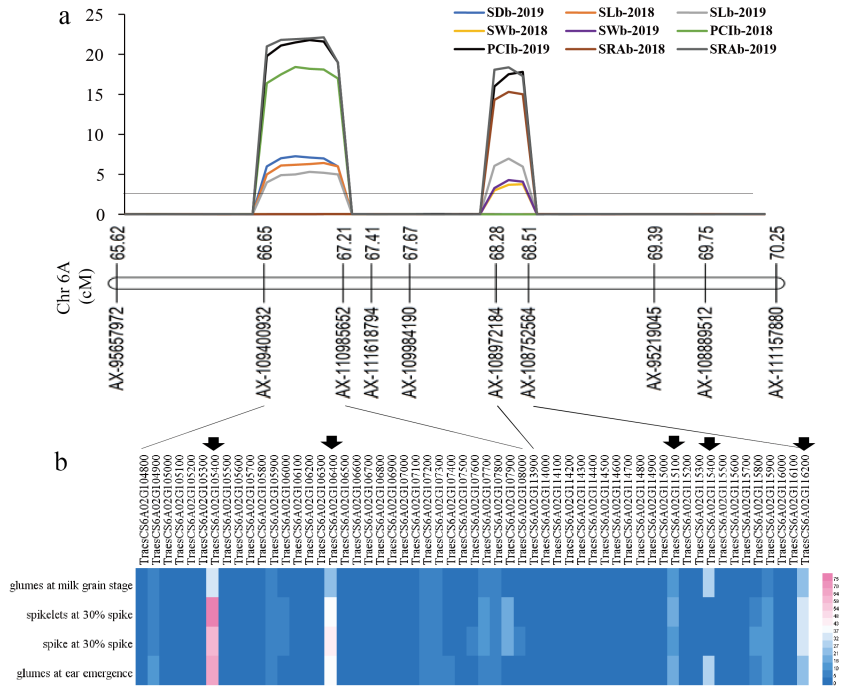

Figure 4 **The locations of two QTL hotspots on chromosome and the candidate genes contained in the two regions.** (A) LOD value of each traits. The line indicates the position where LOD is equal to 2.5. SD, stomatal density; SL, stomatal length; SW, stomatal width; PCI, potential conductance index; SRA, stomatal relative area; b, base of glumes. (B) Heat maps of expression of candidate genes contained in the two regions in wheat spikelets and glumes. The five genes below the black arrow are candidate genes that were screened out in this study.

Full-size DOI: 10.7717/peerj.13262/fig-4

Table 3 **Candidate genes screened from QTL regions in this study.**

Gene ID	Gene annotation
TraesCS6A02G105400	50S ribosomal protein L3
TraesCS6A02G106400	Stress-associated endoplasmic reticulum protein 2
TraesCS6A02G115100	Purple acid phosphatase
TraesCS6A02G115400	Calcium-dependent lipid-binding (CaLB domain) family
TraesCS6A02G116200	ATP-dependent RNA helicase

between stomatal density and stomatal size in wheat leaves (*Wang et al., 2016*). In addition, similar phenomena have been observed in other crops. (*Ishimaru et al., 2001*; *Ohsumi et al., 2007*). The present results showed that stomatal density was negatively correlated with stomatal length in each part of wheat glumes in the two years. However, there was no significant correlation between stomatal density and stomatal width. Previous studies found that stomatal length and stomatal width in wheat leaves were significantly positively correlated (*Wang et al., 2016*). The present results showed that stomatal length and stomatal width were significantly positively correlated in 2018 (Fig. 2 Table S1). Therefore, wheat glumes can improve their adaptability to different environmental

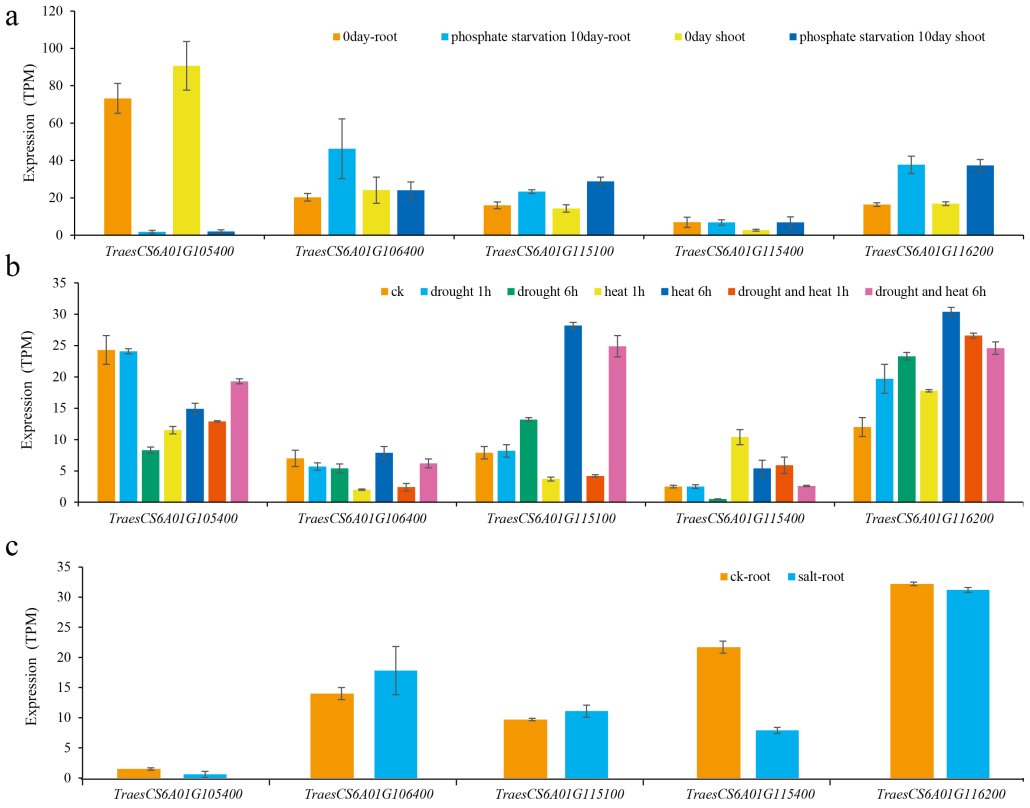

Figure 5 **Expression of candidate genes under various abiotic stresses.** (A) Low phosphorus stress; (B) drought and heat stress; (C) salt stress.

Full-size DOI: 10.7717/peerj.13262/fig-5

conditions by coordinating the relationship among stomatal density, stomatal length, and stomatal width.

Pleiotropy of QTLs for stoma-related traits in wheat

Various studies have found that QTLs of closely related traits may be located on the same or nearby positions on the chromosomes (*Fracheboud et al., 2002*; *Tuberosa et al., 2002*). In the present study, *QSLb-6A*-1 corresponding to stomatal length at the base of glumes, *QSDb-6A* for stomatal density at the base of glumes, *QPCIb-6A-1* for stomatal PCI at the base of glumes, and *QSRAd-6A-1* for stomatal relative area at the base of glumes were detected in the interval of AX-109400932∼AX-110985652 on chromosome 6A in 2018 and 2019. In the vicinity of this interval, *QSWb-6A*, *QSLb-6A*-2, *QPCIb-6A*-2, and *QSRAb-6A*-2 were detected in the interval AX-108972184∼AX-108752564 on chromosome 6A in the two years. *QSDt-5A*, *QSDm-5A*, and *QSRAt-5A* were all located in the interval AX-111662464∼AX-95683796. *QSDt-5D* and *QSLt-5D* were located in the interval Xgwm205.2∼AX-89390905. *QSDm-1A* and *QSLt-1A* were located in the interval AX-111105973∼AX-94402739 (Fig. 3 Table 2).

In addition, compared with previous studies, we found a QTL *QSWt-4B* in this study was located within the region of *QAGsw4B* in the previous study (*Wang et al., 2018*).

QSAb-5A-2 was located within the region of *QAGsd5A*, *QMGsd5A-2*, and *QAGsl5A*. (*Wang et al., 2018*). *QSRAm-5B* was located close to the region of *QPsd5B*, and *QSDd-5A* was located within the region of *QSD5A-2* (*Wang et al., 2016*).

Therefore, the QTLs for above-mentioned stoma-related traits, which were detected in different parts of wheat, different growth periods, and various environments, were significant markers for stoma-related traits in wheat. Furthermore, these findings implied stomatal density and size of wheat leaves and glumes may be controlled by the same or pleiotropic genes. The markers that were localized within a QTL interval associated with stoma-related traits not only validated the QTL but also provided more closely linked markers. These markers will be useful to reveal advanced wheat varieties in wheat breeding programs based on marker-assisted selection approaches.

Prediction of candidate genes related to stomata in wheat glumes

In this study, 57 genes were found in two intervals, AX-109400932∼AX-110985652 (physical range 73571398-76990896 bp) and AX-108972184∼AX-108752564 (physical range 83931623-86272494 bp), on chromosome 6A, and five candidate genes (*i.e.*, *TraesCS6A01G105400*, *TraesCS6A01G106400*, *TraesCS6A02G115100*, *TraesCS6A02G115400*, and *TraesCS6A02G116200*) were screened out, according to their expression levels in wheat glumes or spikes (Fig. 4 Table 3).

The expression level of *TraesCS6A01G105400* in wheat glumes and spikes was the highest among all candidate genes (Fig. 4), and its functional annotation was 50S ribosomal protein L3 (Table 3). The *TraesCS6A01G105400* expression decreased significantly under low phosphorus, drought, and heat stress conditions (Fig. 5). The functional annotation of the candidate gene *TraesCS6A01G106400* is stress-associated endoplasmic reticulum (ER) protein (Table 3). The ER plays a crucial role in the maintenance of cellular homeostasis. ER stress is a widely existed stress mechanism to external stimuli in plants and animals. This pathway maintains the ER homeostasis and alleviates stress damage through regulation of a series of gene expressions (*Park & Park, 2019*). The expression of *TraesCS6A01G106400* was significantly increased under salt stress (Fig. 5). The functional annotation of the candidate gene *TraesCS6A01G115100* is purple acid phosphatase (PAP) (Table 3), and its expression was significantly increased under low phosphorus stress (Fig. 5). PAPs are members of the metallo-phosphoesterase family identified from a wide range of plants. PAPs have mostly been studied for their potential involvement in phosphorus acquisition and redistribution because of their ability to catalyze the hydrolysis of activated phosphate esters and anhydrides under acidic conditions (*Olczak, Morawiecka & Watorek, 2003*). Recent studies also showed that PAPs play important roles in modulating plant carbon metabolism, cell wall synthesis, pathogen resistance, etc (*Kaida et al., 2009*; *Sun et al., 2012*; *Zhang et al., 2014*). *TraesCS6A01G115400* was specifically expressed in wheat glumes, and its functional annotation is calcium-dependent lipid-binding family protein (Table 3). Ca^{2+} is a secondary messenger in plants that regulates virtually all aspects of plant development and responses to environmental stimuli. Ca^{2+} tends to rapidly rise under abiotic stresses (*Bartels & Sunkar, 2005*). Several proteins have been reported to be activated or translocated in the presence of Ca^{2+} including Calcium-dependent

lipid-binding protein (*Hurley & Misra, 2000*). The expression of *TRAESCS6A01G115400* in roots of wheat seedlings was significantly decreased under salt stress (Fig. 5). The functional annotation of the candidate gene *TraesCS6A01G116200* is ATP-dependent RNA helicase (Table 3). ATP-dependent RNA helicase can be found in many organisms, which is involved in the multi-dimensional metabolism of RNA and plays an important role in plant growth and development, especially in abiotic stress response (*Kim et al., 2008*). The expression of *TraesCS6A01G116200* was significantly increased under low phosphorus, drought, and heat stress (Fig. 5).

The above five candidate genes not only had high expression levels in wheat glumes or spikes, but are also induced by a variety of abiotic stresses. Studies have shown that when plants are subjected to abiotic stress, they can change their photosynthetic rate and transpiration rate by adjusting the stomata size, stomata density, and stomata distribution to deal with bad external environments (*Doheny-Adams et al., 2012*; *Franks et al., 2015*). Therefore, it will be greatly helpful to analyze whether these five genes affect the formation of wheat stomata through transgenic experiments in future research, and to explore the mechanism of their functions.

CONCLUSION

In this study, a total of 61 QTLs for traits related to stomata of wheat glumes were identified in the two years, which were distributed across 16 chromosomes and explained 3.63–19.02% of phenotypic variation. Among them, two QTL hotspots were found in 6A, including four and four QTLs, respectively. Subsequently, five candidate genes were screened out, according to their expression levels in wheat glumes or spikes. The expression of these genes could be induced by a variety of abiotic stresses. Our results provide insights for cloning and functional characterization of stoma-related candidate genes in wheat glumes.

ACKNOWLEDGEMENTS

We gratefully acknowledge the anonymous reviewers for their constructive comments. We would also like to thank TopEdit for its linguistic assistance during the preparation of this manuscript.

ADDITIONAL INFORMATION AND DECLARATIONS

Funding

This work was funded by the Science & Technology Innovation Foundation of Shanxi Agricultural University (2020BQ30) and the Outstanding Doctor Funding Award of Shanxi Province (SXYBKY2019040). The funders had no role in study design, data collection and analysis, decision to publish, or preparation of the manuscript.

Grant Disclosures

The following grant information was disclosed by the authors:

Science & Technology Innovation Foundation of Shanxi Agricultural University: 2020BQ30.
Outstanding Doctor Funding Award of Shanxi Province: SXYBKY2019040.

Competing Interests

The authors declare there are no competing interests.

Author Contributions

- Ning Li conceived and designed the experiments, performed the experiments, analyzed the data, prepared figures and/or tables, authored or reviewed drafts of the paper, and approved the final draft.
- Fanfan Dong and Tongtong Liu performed the experiments, analyzed the data, prepared figures and/or tables, and approved the final draft.
- Jinwen Yang and Shuguang Wang analyzed the data, prepared figures and/or tables, and approved the final draft.
- Yugang Shi analyzed the data, prepared figures and/or tables, authored or reviewed drafts of the paper, and approved the final draft.
- Daizhen Sun and Ruilian Jing conceived and designed the experiments, authored or reviewed drafts of the paper, and approved the final draft.

Data Availability

The following information was supplied regarding data availability:

The raw measurements are available in the Supplementary File.

Supplemental Information

Supplemental information for this article can be found online at http://dx.doi.org/10.7717/peerj.13262#supplemental-information.

REFERENCES

Aasamaa K, Sober A, Rahi M. 2001. Leaf anatomical characteristics associated with shoot hydraulic conductance, stomatal conductance, and stomatal sensitivity to changes of leaf water status in temperate deciduous trees. *Australia Journal of Plant Physiology* **28**:765–774 DOI 10.1071/PP00157.

Abbad H, Jaafari SE, Bort J, Araus JL. 2004. Comparison of flag leaf and ear photosynthesis with biomass and grain yield of durum wheat under various water conditions and genotypes. *Agronomie* **24**:19–28 DOI 10.1051/agro:2003056.

Aliyev JA. 2012. Photosynthesis, photorespiration and productivity of wheat and soybean genotypes. *Physiologia Plantarum* **145**:369–383 DOI 10.1111/j.1399-3054.2012.01613.x.

Araus JL, Bort J, Brown HR, Bassett C, Cortadellas N. 1993. Immunocytochemical localization of phosphoenolpyruvate carboxylase and photosynthetic gas exchange characteristics in ears of *Triticum durum* Desf. *Planta* **191**:507–514.

Bartels D, Sunkar R. 2005. Drought and salt tolerance in plants. *Critical Reviews in Plant Sciences* **24**:23–58 DOI 10.1080/07352680590910410.

Berger D, Altmann T. 2000. A subtilisin-like serine protease involved in the regulation of stomatal density and distribution in Arabidopsis thaliana. *Genes and Development* **14**:1119–1131 DOI 10.1101/gad.14.9.1119.

Boccalandro HE, Rugnone ML, Moreno JE, Ploschuk EL, Serna L, Yanovsky MJ, Casal JJ. 2009. Phytochrome b enhances photosynthesis at the expense of water-use efficiency in Arabidopsis. *Plant Physiology* **150**:1083–1092 DOI 10.1104/pp.109.135509.

Doheny-Adams T, Hunt L, Franks PJ, Beerling DJ, Gray JE. 2012. Genetic manipulation of stomatal density influences stomatal size, plant growth and tolerance to restricted water supply across a growth CO_2 gradient. *Philosophical Transactions of the Royal Society B: Biological Sciences* **367**:547–555 DOI 10.1098/rstb.2011.0272.

Fracheboud Y, Ribaut JM, Vargas M, Mesamer R, Stamp P. 2002. Identification of quantitative trait loci for cold tolerance of photosynthesis in maize (*Zea mays* L.). *Journal of Experimental Botany* **53**:1967–1977 DOI 10.1093/jxb/erf040.

Franks PJ, Beerling DJ. 2009. Maximum leaf conductance driven by CO_2 effects on stomatal size and density over geologic time. *Proceedings of the National Academy of Sciences of the United States of America* **106**:10343–10347 DOI 10.1073/pnas.0904209106.

Franks PJ, Doheny-Adams TW, Britton-Harper ZJ, Gray JE. 2015. Increasing water-use efficiency directly through genetic manipulation of stomatal density. *New Phytologist* **207**:188–195 DOI 10.1111/nph.13347.

Gebbing T, Schnyder H. 2001. 13C Labeling kinetics of sucrose in glumes indicates significant refixation of respiratory CO_2 in the wheat ear. *Functional Plant Biology* **28**:1047–1053 DOI 10.1071/PP01072.

Hu HH, Boisson-Dernier A, Israelsson NM, Böhmer M, Xue SW, Ries A, Godoski J, Kuhn JM, Schroeder JI. 2010. Carbonic anhydrases are upstream regulators in guard cells of CO_2-controlled stomatal movements. *Nature Cell Biology* **12**:87–93 DOI 10.1038/ncb2009.

Hurley JH, Misra S. 2000. Signaling and subcellular targeting by membrane-binding domains. *Annual Review of Biophysics and Biomolecular Structure* **29**:49–79 DOI 10.1146/annurev.biophys.29.1.49.

Ishimaru K, Shirota K, Higa M, Kawamitsu Y. 2001. Identification of quantitative trait loci for adaxial and abaxial stomatal frequencies in *Oryza sativa*. *Plant Physiology and Biochemistry* **39**:173–177 DOI 10.1016/S0981-9428(00)01232-8.

Kaida R, Satoh Y, Bulone V, Yamada Y, Kaku T, Hayashi T, Kaneko TS. 2009. Activation of β-glucan synthases by wall-bound purple acid phosphatase in tobacco cells. *Plant Physiology* **150**:1822–1830 DOI 10.1104/pp.109.139287.

Kim JS, Kim KA, Oh TR, Park CM, Kang H. 2008. Functional characterization of DEAD-box RNA helicases in Arabidopsis thaliana under abiotic stress conditions. *Plant and Cell Physiology* **49**:1563–1571 DOI 10.1093/pcp/pcn125.

Knoppik D, Selinger H, Ziegler-Jöns A. 1986. Differences between the flag leaf and of ear of a spring wheat cultivar (*Triticum aestivum* cv. Arkas) with respect to the CO_2 response of assimilation, respiration and stomatal conductance. *Physiologia Plantarum* **68**:451–457 DOI 10.1111/j.1399-3054.1986.tb03381.x.

Kong LA, Wang FH, Feng B, Li SD, Si JS, Zhang B. 2010. The structural and photosynthetic characteristics of the exposed peduncle of wheat (*Triticum aestivum* L.): an important photosynthate source for grain-filling. *BMC Plant Biology* **10**:141 DOI 10.1186/1471-2229-10-141.

Laza MRC, Kondo M, Ideta O, Barlaan E, Imbe T. 2010. Quantitative trait loci for stomatal density and size in lowland rice. *Euphytica* **172**:149–158 DOI 10.1007/s10681-009-0011-8.

Li L, Mao XG, Wang JY, Chang XP, Reynolds M, Jing RL. 2019. Genetic dissection of drought and heat-responsive agronomic traits in wheat. *Plant Cell and Environment* **42**:2540–2553 DOI 10.1111/pce.13577.

Li L, Peng Z, Mao XG, Wang JY, Li CN, Chang XP, Jing RL. 2021. Genetic insights into natural variation underlying salt tolerance in wheat. *Journal of Experimental Botany* **72**:1135–1150 DOI 10.1093/jxb/eraa500.

Li YP, Li HB, Li YY, Zhang SQ. 2017. Improving water-use efficiency by decreasing stomatal conductance and transpiration rate to maintain higher ear photosynthetic rate in drought-resistant wheat. *The Crop Journal* **5**:231–239 DOI 10.1016/j.cj.2017.01.001.

Liu XL, Li RZ, Chang XP, Jing RL. 2013. Mapping QTLs for seedling root traits in a doubled haploid wheat population under different water regimes. *Euphytica* **189**:51–66 DOI 10.1007/s10681-012-0690-4.

Liu ZS, Xin MM, Qin XJ, Peng HR, Ni ZF, Yao YY, Sun QX. 2015. Temporal transcriptome profiling reveals expression partitioning of homeologous genes contributing to heat and drought acclimation in wheat (*Triticum aestivum* L.). *BMC Plant Biology* **15**:152 DOI 10.1186/s12870-015-0511-8.

Lopes MS, Cortadellas N, Kichey T, Dubois F, Habash DZ, Araus JL. 2006. Wheat nitrogen metabolism during grain filling: comparative role of glumes and the flag leaf. *Planta* **225**:165–181 DOI 10.1007/s00425-006-0338-5.

Ma SW, Wang M, Wu JH, Guo WL, Chen YM, Li GW, Wang YP, Shi WM, Xia GM, Fu DL, Kang ZS, Ni F. 2021. WheatOmics: a platform combining multiple omics data to accelerate functional genomics studies in wheat. *Molecular Plant* **14**:1965–1968 DOI 10.1016/j.molp.2021.10.006.

Maydup ML, Antonietta M, Guiamet JJ, Graciano C, López JR, Tambussi EA. 2010. The contribution of ear photosynthesis to grain filling in bread wheat (*Triticum aestivum* L.). *Field Crops Research* **119**:48–58 DOI 10.1016/j.fcr.2010.06.014.

Nazanin A, Ahmad I, Mohammad RG, Farhad NF, Shobbar ZS. 2019. Transcriptome response of roots to salt stress in a salinity-tolerant bread wheat cultivar. *PLOS ONE* **14**:3.

Nicholas H, Richardson AD. 2009. Stomatal length correlates with elevation of growth in four temperate species. *Journal of Sustainable Forestry* **28**:63–73 DOI 10.1080/10549810802626142.

Ohsumi A, Kanemura T, Homma K, Horie T, Shiraiwa T. 2007. Genotypic variation of stomatal conductance in relation to stomatal density and length in rice (*Oryza sativa* L.). *Plant Production Science* **10**:322–328 DOI 10.1626/pps.10.322.

Olczak M, Morawiecka B, Watorek W. 2003. Plant purple acid phosphatases-genes, structures and biological function. *Acta Biochimica Polonica* **50**:1245–1256 DOI 10.18388/abp.2003_3648.

Oono Y, Kobayashi F, Kawahara Y, Yazawa T, Handa H, Itoh T, Matsumoto T. 2013. Characterisation of the wheat (triticum aestivum L.) transcriptome by de novo assembly for the discovery of phosphate starvation-responsive genes: gene expression in Pi-stressed wheat. *BMC Genomics* **14**:77 DOI 10.1186/1471-2164-14-77.

Park CJ, Park JM. 2019. Endoplasmic reticulum plays a critical role in integrating signals generated by both biotic and abiotic stress in plants. *Frontiers in Plant Science* **10**:399 DOI 10.3389/fpls.2019.00399.

Qi X, Torii KU. 2018. Hormonal and environmental signals guiding stomatal development. *BMC Biology* **16**:21 DOI 10.1186/s12915-018-0488-5.

Robert RW, Gretchen FS, Richard GP. 2000. A comparison of leaf anatomy in field-grown gossypium hirsutum and G. barbadense. *Annals of Botany* **86**:731–738 DOI 10.1006/anbo.2000.1235.

Rubén V, Omar VD, Susan M, Fadia C, Shawn CK, Jordi B, María DS, Nieves A, José LA. 2018. Durum wheat ears perform better than the flag leaves under water stress: gene expression and physiological evidence. *Environmental and Experimental Botany* **153**:271–285 DOI 10.1016/j.envexpbot.2018.06.004.

Sánchez-Bragado R, Molero G, Reynolds MP, Araus JL. 2014. Relative contribution of shoot and ear photosynthesis to grain filling in wheat under good agronomical conditions assessed by differential organ δ^{13}C. *Journal of Experimental Botany* **65**:5401–5413 DOI 10.1093/jxb/eru298.

Sánchez-Díaz M, García JL, Antolín MC, Araus JL. 2002. Effects of soil drought and atmospheric humidity on yield, gas exchange, and stable carbon composition of barley. *Photosynthetica* **40**:415–421 DOI 10.1023/A:1022683210334.

Shi HW, Guan WH, Shi YG, Wang SG, Fan H, Yang JW, Chen WG, Zhang WJ, Sun DZ, Jing RL. 2020. QTL mapping and candidate gene analysis of seed vigor-related traits during artificial aging in wheat (*Triticum aestivum*). *Scientific Reports* **10**:22060 DOI 10.1038/s41598-020-75778-z.

Stephens J, Waugh R. 2017. Reducing stomatal density in barley improves drought tolerance without impacting on yield. *Plant Physiology* **174**:776–787 DOI 10.1104/pp.16.01844.

Sun JG, Liu CC, Hou JH, He NP. 2021. Spatial variation of stomatal morphological traits in grassland plants of the Loess Plateau. *Ecological Indicators* **128**:107857 DOI 10.1016/j.ecolind.2021.107857.

Sun F, Suen PK, Zhang YJ, Sun F, Suen PK, Zhang YJ, Liang C, Carrie C, Whelan J, Ward JL, Hawkins ND, Jiang LW, Lim BL. 2012. A dual-targeted purple acid phosphatase in Arabidopsis thaliana moderates carbon metabolism and its overexpression leads to faster plant growth and higher seed yield. *New Phytologist* **194**:206–219 DOI 10.1111/j.1469-8137.2011.04026.x.

Tambussi EA, Bort J, Guiamet JJ, Nogués S, Araus JL. 2007. The photosynthetic role of ears in C3 cereals: metabolism, water use efficiency and contribution to grain yield. *Critical Reviews in Plant Sciences* **26**:1–16 DOI 10.1080/07352680601147901.

Tambussi E, Nogues SJ. 2005. Ear of durum wheat under water stress: water relations and photosynthetic metabolism. *Planta* **221**:446–458 DOI 10.1007/s00425-004-1455-7.

Teng S, Qian Q, Zeng DL, Kunihiro Y, Fujimoto K, Huang DN, Zhu LH. 2004. QTL analysis of leaf photosynthetic rate and related physiological traits in rice (*Oryza sativa L.*). *Euphytica* **135**:1–7 DOI 10.1023/B:EUPH.0000009487.89270.e9.

The International Wheat Genome Sequencing Consortium (IWGSC). 2018. Shifting the limits in wheat research and breeding using a fully annotated reference genome. *Science* **361**:eaar7191 DOI 10.1126/science.aar7191.

Tuberosa R, Salvi S, Sanguineti MC, Landi P, Maccaferri M, Conti S. 2002. Mapping QTL regulating morphophysiologyical traits and yield: Case studies, shortcomings and perspectives in drought stressed maize. *Annals of Botany* **89**:941–963 DOI 10.1093/aob/mcf134.

Wang SG, Dong FF, Sun DZ, Chen YY, Yan X, Jing RL. 2018. QTL analysis for stomatal density and size in wheat spike organ. *Emirates Journal of Food and Agriculture* **30**:173–179.

Wang SG, Jia SS, Sun DZ, Fan H, Chang XP, Jing RL. 2016. Mapping QTLs for stomatal density and size under drought stress in wheat (*Triticum aestivum L*). *Journal of Integrative Agriculture* **9**:1955–1967.

Wang ZM, Wei AL, Zheng DM. 2001. Photosynthetic characteristics of non-leaf organs of winter wheat cultivars differing in ear type and their relationship with grain mass per ear. *Photosynthetica* **39**:239–244 DOI 10.1023/A:1013743523029.

Wardlaw IF. 2002. Interaction between drought and chronic high temperature during kernel filling in wheat in a controlled environment. *Annals of Botany* **90**:469–476 DOI 10.1093/aob/mcf219.

Wei TY, Simko V. 2013. Corrplot: visualization of a correlation matrix, MMWR. *Mmwr Morbidity and Mortality Weekly Report* **52**:145–151.

Zhang YJ, Sun F, Fettke J, Schöttler MA, Ramsden L, Fernie AR, Lim BL. 2014. Heterologous expression of AtPAP2 in transgenic potato influences carbon metabolism and tuber development. *FEBS Letters* **588**:3726–3731 DOI 10.1016/j.febslet.2014.08.019.

Zhou BW, Sanz-Sáez Á, Elazab A, Shen TM, Sánchez-Bragado R, Bort J, Serret DM, Araus JL. 2014. Physiological traits contributed to the recent increase in yield potential of winter wheat from Henan Province, China. *Journal of Integrative Plant Biology* **56**:492–504 DOI 10.1111/jipb.12148.

Zhu CX, Zhu JG, Zeng Q, Liu G, Xie ZB, Tang HY, Cao JL, Zhao XZ. 2009. Elevated CO^2 accelerates flag leaf senescence in wheat due to ear photosynthesis which causes greater ear nitrogen sink capacity and ear carbon sink limitation. *Functional Plant Biology* **36**:291–299 DOI 10.1071/FP08269.